

Fig. 1. Polarization curves for carbon steel in 1 M HCl in the absence and presence of different concentrations of inhibitor (AS-Zn) at 25 °C.

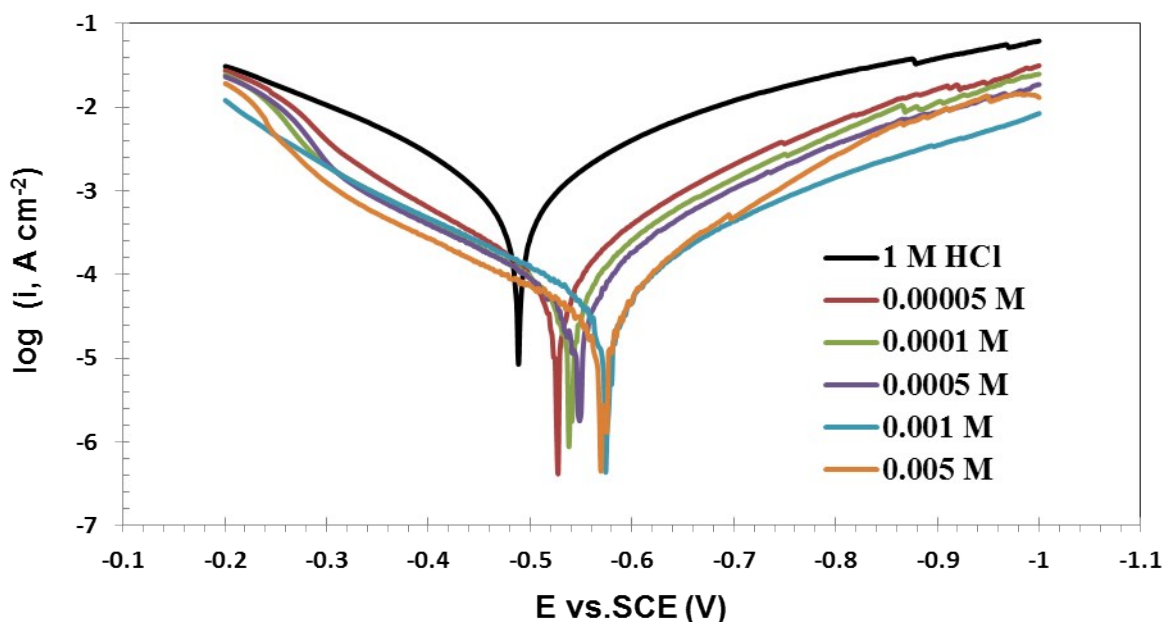


Fig. 2. Polarization curves for carbon steel in 1 M HCl in the absence and presence of different concentrations of inhibitor (AS-Co) at 25 °C.

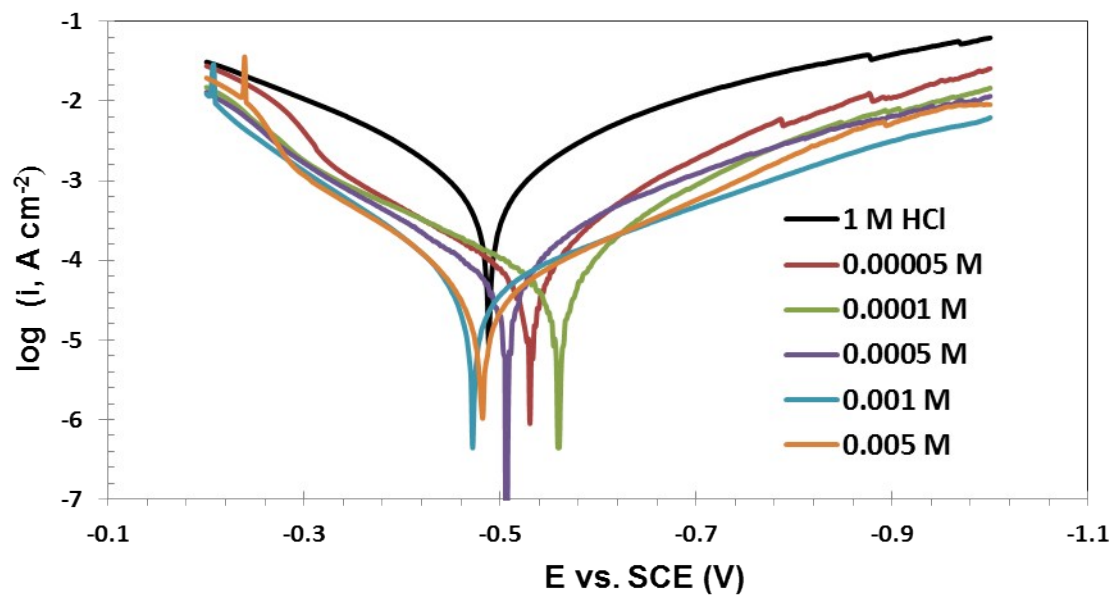


Fig. 3. Polarization curves for carbon steel in 1 M HCl in the absence and presence of different concentrations of inhibitor (AS-Cu) at 25 °C.

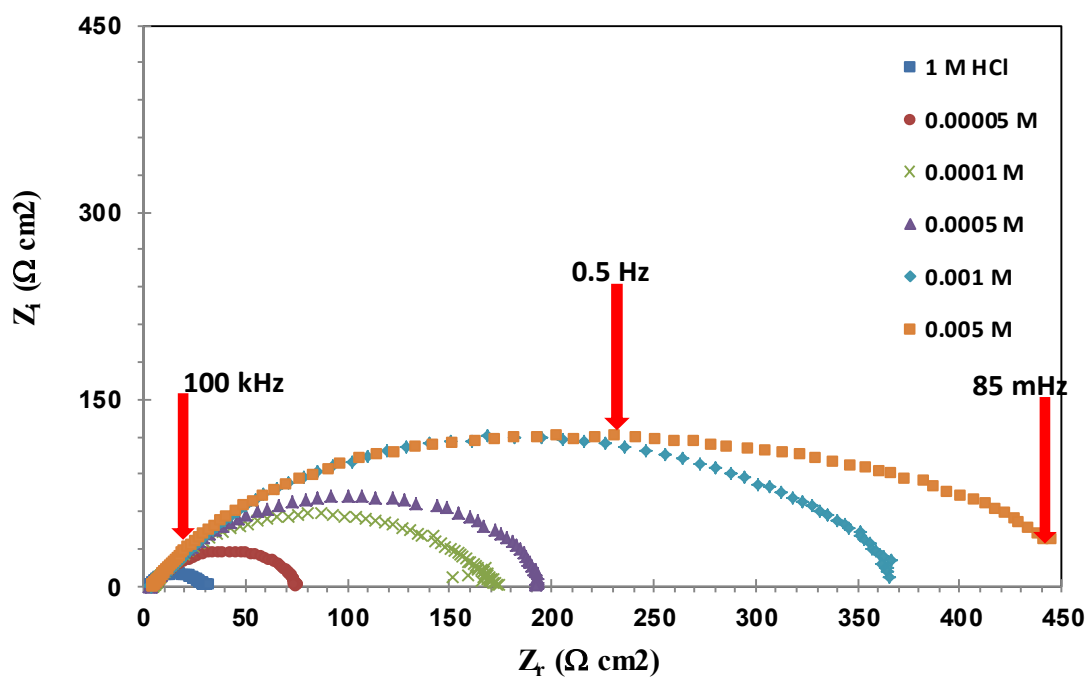


Fig. 4. Nyquist plots for CS in 1 M HCl in absence and presence of different concentrations of inhibitor (AS-Zn) at 25 °C

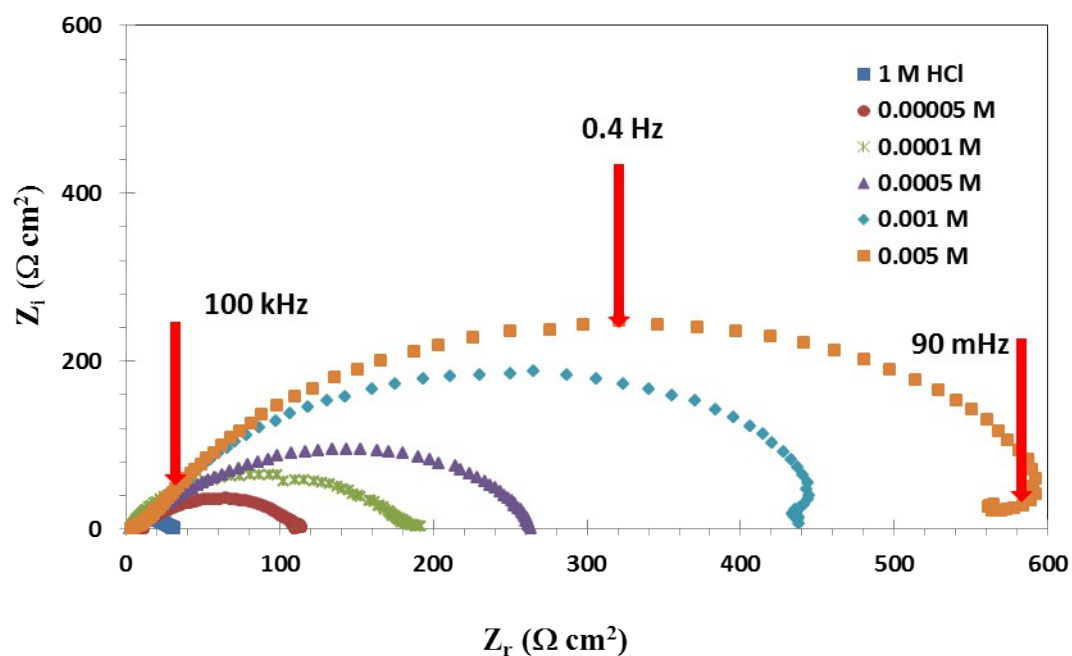


Fig. 5. Nyquist plots for CS in 1 M HCl in absence and presence of different concentrations of inhibitor (AS-Co) at 25 °C

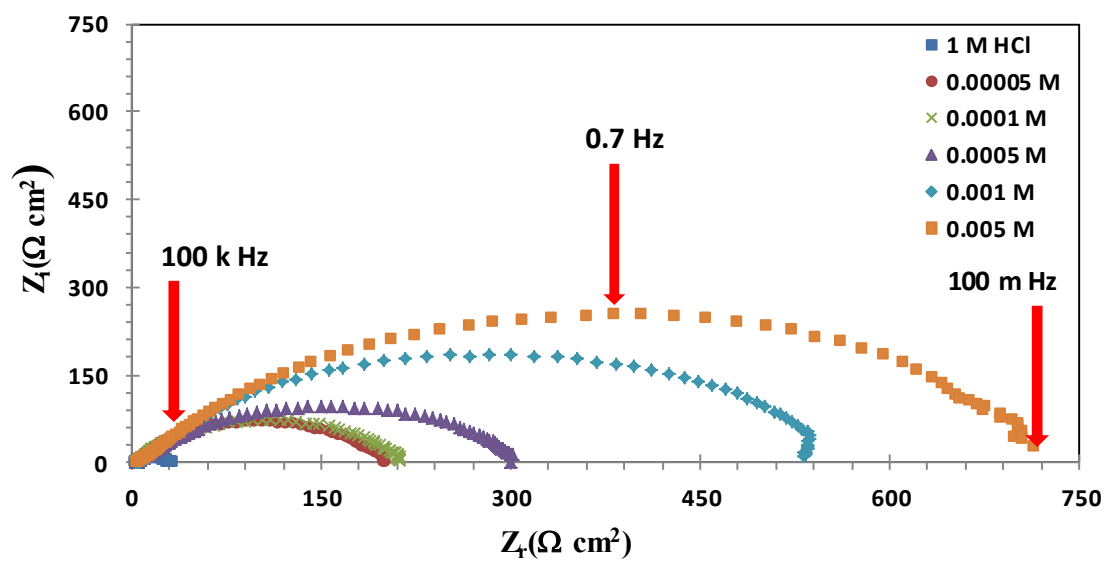


Fig. 6. Nyquist plots for CS in 1 M HCl in absence and presence of different concentrations of inhibitor (AS-Cu) at 25 °C

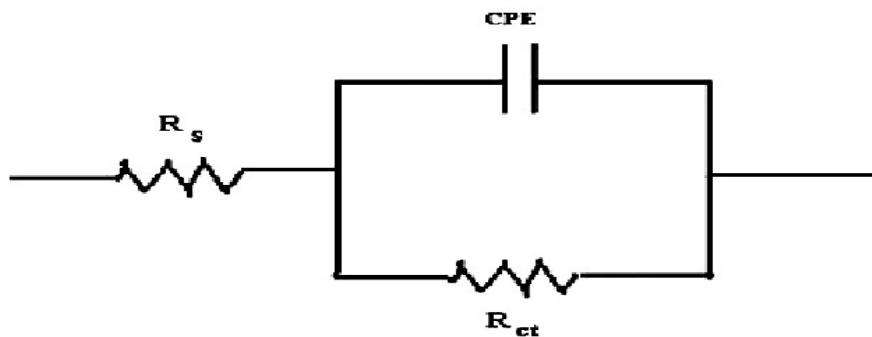


Fig. 7. Electrical equivalent circuit used for modeling the interface Fe/1 M HCl solution without and with the synthesized surfactant inhibitors.

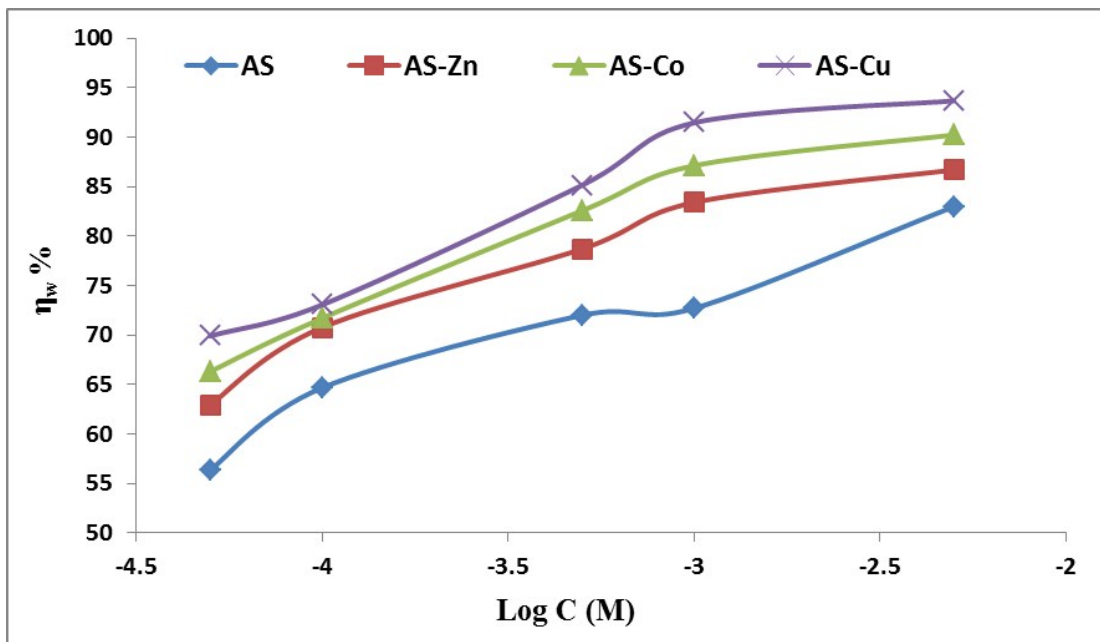


Fig. 8. Variation of the inhibition efficiency with different concentrations of the synthesized inhibitors in 1 M HCl at 25 °C.

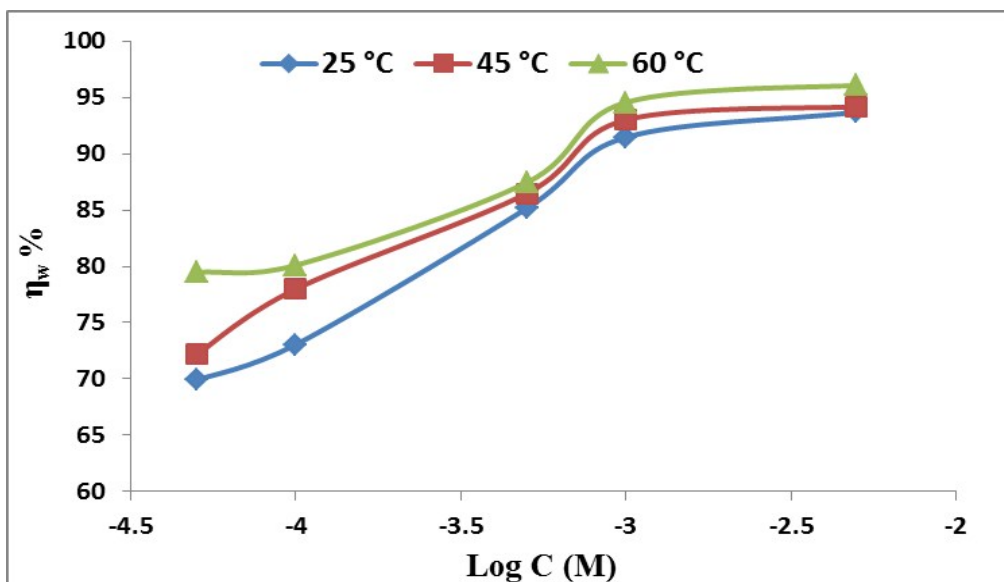
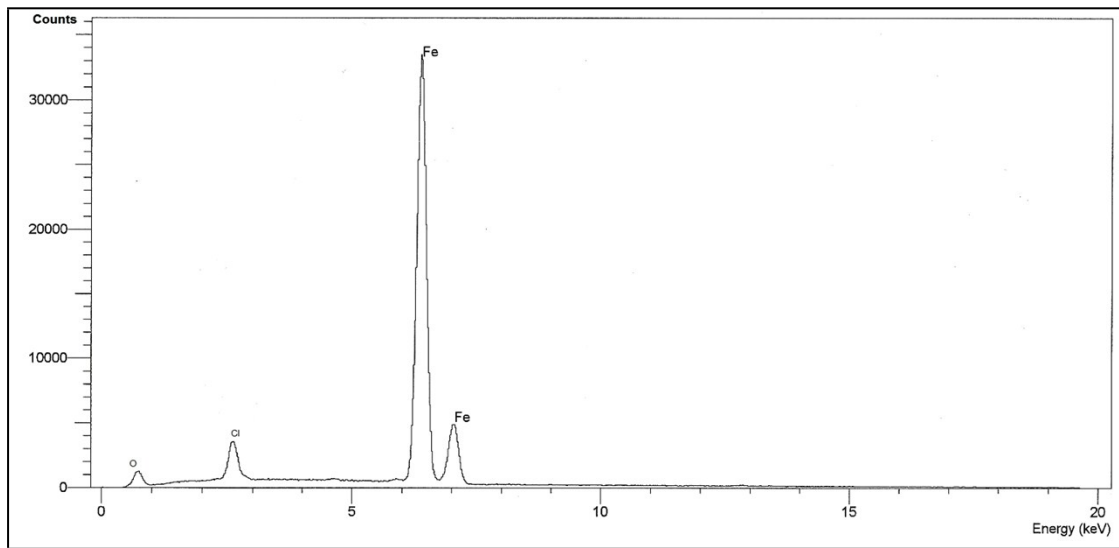
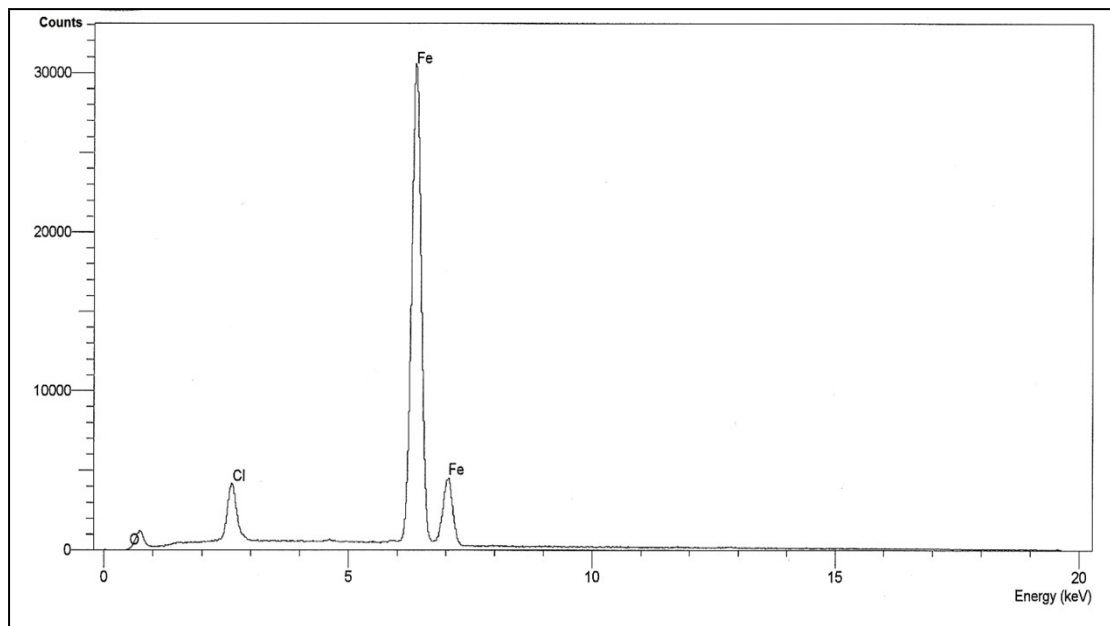


Fig. 9. Effect of the temperature on the inhibition efficiency was obtained by weight loss method for carbon steel in 1 M HCl in presence of different concentrations of inhibitor (AS-Cu).

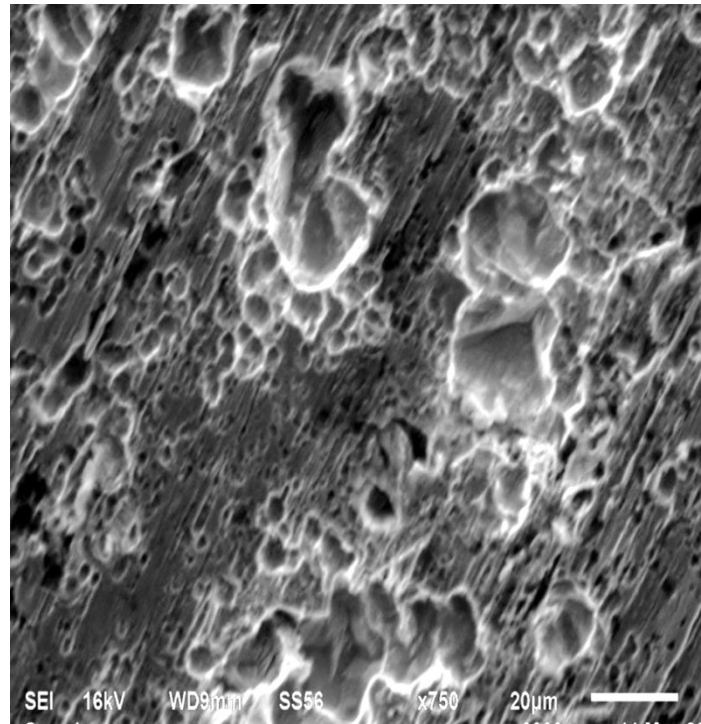


(a)

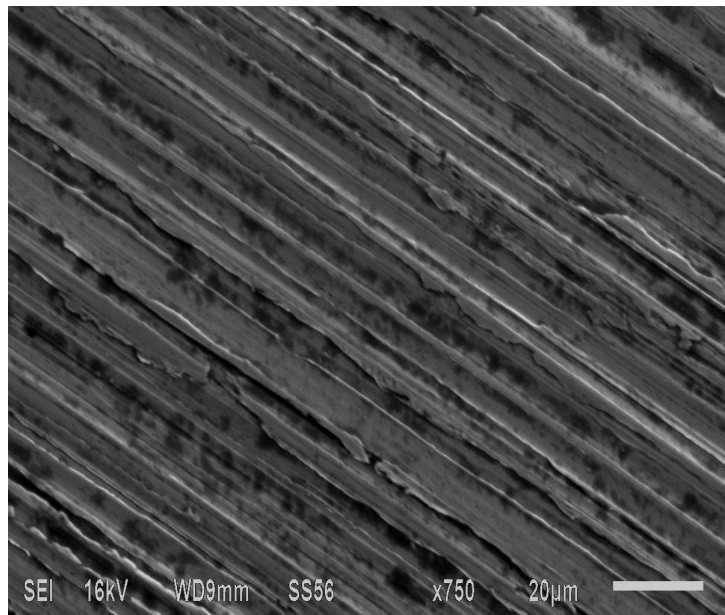


(b)

Fig. (10): (a) The EDX spectrum of carbon steel in uninhibited 1.0 M HCl, (b) in presence of 5×10^{-3} M of synthesized alginate surfactant (AS-Cu) in 1.0 M HCl.



(a)



(b)

Fig. 11. SEM image of surface of carbon steel after immersion for 24 h in 1 M HCl at 25 °C in absence (a) and presence of 5×10^{-3} M of AS-Cu(b)